Nonlinear Model Predictive Control for Thermal Management of Bio-Implants

Ayca Ermis, Yen-Pang Lai and Ying Zhang

Abstract— **Thermal management of bio-implant and implantable medical devices (IMDs) has gained growing attention to prevent overheating in the surrounding tissue of IMDs in certain applications, such as neural prostheses like deep brain stimulators (DBS). This paper focuses on implementation of nonlinear model predictive control (NMPC) methods for adaptive thermal management of IMDs with multiple heat sources. Thermal dynamics of the IMD is modelled using an identification algorithm introduced in previous papers. Interior point optimization method is implemented with the NMPC to solve for the nonlinear optimization problem for adaptive thermal management of IMDs with multiple heat sources. The NMPC implementation is validated using the COMSOL software simulations.**

I. INTRODUCTION

Improved functionalities of implantable medical devices (IMDs), such as monitoring, recording neural signals and providing stimulation etc. lead to more power consumption which may cause damage in the surrounding tissue due to overheating of the electrodes. Cases of overheating and tissue damage in various applications of IMDs have been discussed in [1]-[3]. Thus, specifically for the neural IMDs, low power consumption and real-time thermal management of these devices are of great importance to maintain the long-term operation of the device while ensuring patient's health and safety.

Various nonlinear model predictive control (NMPC) algorithms have been explored in previous literature with very few applications to thermal management problem. Diehl et al. surveyed various Newton-type optimization methods and algorithms used to solve real-time optimal control problems, such as NMPC and moving horizon estimation (MHE) in [4]. In [5], authors design a position controller for quadrotors using the NMPC algorithm with real-time iteration (RTI) scheme to compensate for time-delay. Both in [6] and [7], economic NMPC (ENMPC) scheme is investigated. In [6], an ENMPC scheme with Moving Horizon Estimation (MHE) algorithm for state estimation is implemented to achieve real-time power maximization of wind turbine generators, whereas in [7], authors implement an ENMPC scheme using reinforcement learning tools for tuning. In both of these works, authors provide simulation results for evaluation of the NMPC performance.

This work was supported in part by the National Science Foundation under Grant ECCS-1711447.

Ayca Ermis and Yen-Pang Lai are PhD students in the School of Electrical and Computer Engineering, Georgia Tech, Atlanta, GA 30332, USA. aycaermis@gatech.edu, yenpang_lai@gatech.edu

Ying Zhang is with the School of Electrical and Computer Engineering, Georgia Tech, Atlanta, GA 30332, USA. yzhang@gatech.edu

For adaptive thermal management applications, there have been few studies focusing on model predictive control methods. In [8], an NMPC method is proposed for thermal management in plug-in hybrid electric vehicles which focuses on minimizing thermal stress and electrical consumption. Specifically for adaptive thermal management problem of IMDs, in [9], an on-off control approach is adopted to operate the device at maximum power levels until a set temperature is reached. Once the set temperature is reached, the adopted control loop puts the device in sleep mode. In [10], a proportional-integral-derivative (PID) controller is implemented for active charge balancing to ensure a safe neural stimulation. A simplified electrode model is used to evaluate the performance of the PID controller proposed. Alternatively, in [11], authors integrate a model predictive control scheme with a simplified single-input single-output thermal model for the adaptive thermal management of IMDs. However, for the IMDs with multiple heat sources, i.e. multiple modules contributing to the temperature increase of the device, a more complex system identification algorithm, such as the modeling algorithm proposed in [12], is necessary to accurately model the thermal dynamics of the IMD. To the authors' knowledge, there have not been any studies implementing NMPC scheme for adaptive thermal management problem of implantable medical devices with multiple heat sources.

In this paper, nonlinear model predictive methods are investigated for integration with the modeling algorithm previously proposed in [12] and a nonlinear model predictive control scheme with interior point optimization method is implemented with this algorithm for the real-time thermal management of IMDs to ensure safe operation while optimizing power consumption and device performance. The goal of the nonlinear model is to accurately model the heat dissipation due to on-board and external modules, such as wireless power transmission, energy storage device and power circuitry and so on. Thus, due to the spatially distributed nature of these modules, the overall system becomes a multiple-input multiple-output system with nonlinearities. The thermal dynamics of the IMDs with multiple heat sources is modeled with our online identification algorithm which considers the spatial distribution of heat dissipation and its effect on the temperature increase when solving for the model parameters. Further explanation on our online prediction algorithm can be found in [12]. The NMPC scheme with interior point method implemented in this paper is validated via simulation studies using the COMSOL software.

This paper is organized as follows. Section II presents the IMD system model and the prediction algorithm used in this paper. In Section III, formulation of the NMPC scheme with interior-point method is explained. Simulation results and comparison results to the dual control scheme in [9] are presented in Section IV. Lastly, conclusion and future works are discussed in Section V.

II. SYSTEM DESCRIPTION & MODEL

In order to evaluate the performance of the nonlinear control scheme with the identification algorithms, Utah Electrode Array (UEA) is chosen since its thermal effect has been studied in previous works [13], [14]. The UEA consists of multiple modules, such as radio module for wireless communication, motherboard module consisting of the microcontroller (MCU), and power circuitry. The thermal management test vehicle (TMTV) developed based on the UEA consists of multiple heat sources and multiple heat sensors which are spatially distributed on the board. Systems inputs are the power inputs to the heat sources and outputs are temperature readings at sensor locations, thus the overall system is a multiple-input multiple-output system. A diagram of the system and a breakdown of the prediction algorithm are shown in Figure 1.

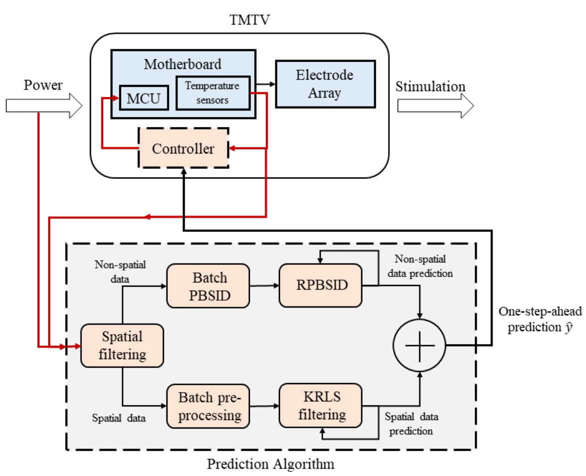

Fig. 1: System diagram.

Using the identification algorithm introduced in [12], the nonlinear system model can be denoted as

$$\hat{x}_{k+1} = f(x_k, u_k) \tag{1}$$

where u_k is a $l \times 1$ vector of model inputs, x_k is a $r \times 1$ vector of the model outputs, $\hat{x}_{k+1}$ is a $r \times 1$ vector of the prediction of model outputs at time instant $k+1$. $f(.)$ stands for the nonlinear prediction algorithm from [12]. The prediction algorithm adopted in [12] uses spatial filtering, kernel recursive least squares filters, and recursive subspace identification methods for predicting the one-step-ahead temperature readings. Due to the nonlinearities introduced by the identification algorithm, a nonlinear model predictive control algorithm is chosen to be implemented for the adaptive thermal management problem.

A. *Online Identification Algorithm*

The identification algorithm introduced in [12] applies a novel spatial filtering to to separate the data into its spatially dependent and independent components and predicts the one-step-ahead value of the non-spatial and spatial data components using recursive predictor-based subspace identification (RPBSID) methods and kernel recursive least squares (KRLS) methods, respectively.

At any time instant, the data could be filtered into its non-spatial and spatial components as follows:

$$\begin{aligned} x^{ns} &= \frac{1}{r(r-1)} \sum_i \sum_j \frac{w_{ij} x_i}{G_i(d)} \\ x^s &= x - x^{ns} \end{aligned} \tag{2}$$

where $G_i(d)$ is the local Getis-Ord statistic, w_{ij} is the element of the $r \times r$ spatial weights matrix. The spatial weights matrix is constructed to represent the correlation between the different sensor locations and the spatial heat dissipation of the heat sources at these sensor locations [12].

For the non-spatial data component, the one-step-ahead predictor can be written using a vector autoregressive model with exogenous inputs (VARX) predictor as:

$$\hat{x}^{\mathrm{ns}}_{k+1|k} = \bar{\Xi}_k \theta_{k+1} + e_k \tag{3}$$

where $\theta_{k+1} = \left[{u_p}^T, \quad {u_{k+1}}^T, \quad {x_p}^T \right]^T$, u_p and x_p are the vectors of past p data points at time instant $k+1$. There exists three matrices, $\bar{\Xi}_k$, error covariance matrix P_k, and the selection matrix S_k, which are updated iteratively with a recursive least squares (RLS) filter. System matrices A, B, C, D, and the Kalman gain K are then computed by updating the corresponding RLS filters [12], [15]. These system matrices can then be used to predict the non-spatial component at $k+1$ as follows:

$$\hat{x}^{\mathrm{ns}}_{k+1|k} = C_k \bar{x}^{ns}_k + D_k u_k \tag{4}$$

where $\bar{x}^{\mathrm{ns}}_k$ is the state vector which is updated by $\bar{x}^{\mathrm{ns}}_{k+1} = A_k \bar{x}^{\mathrm{ns}}_k + B_k u_k + (x^{\mathrm{ns}}_k - \hat{x}^{\mathrm{ns}}_k)$.

Prior to recursive prediction of $\hat{x}^{\mathrm{ns}}_{k+1|k}$, initial values for system matrices and the Kalman gain is calculated using a training data set via regularized batch processing (batch PBSID) as described in [12].

For the spatial data component, the one-step-ahead predictor can be written as a nonlinear pure spatially lagged autoregressive (SAR) model using a kernel recursive least squares (KRLS) filter with a Gaussian kernel as follows:

$$\hat{x}^s_{k+1|k} = \sum_{i=1}^{m_k} \rho_i \exp\left(- \frac{\|\hat{\psi}_{k,i} - \psi_k\|^2}{2\sigma^2} \right) \tag{5}$$

where $\psi_k = W_k x^s_k$ with $r \times 1$ stacked vector of spatial data components of each sensor location $i = 1, \ldots, r$, $(\rho_1, \ldots, \rho_{m_k})$ are the kernel weights, and ε_k is the $r \times 1$ prediction error vector. Additionally, $\hat{\psi}_{k,i}$ for $i, 1 \ldots, m_k$ are the vectors in the dictionary $D_k = \{(\hat{\psi}_i, \hat{x}_i)\}_{i=1}^{m_k}$, and m_k denotes the number of data points admitted to the dictionary. The dictionary D_k is admits new data if and only if the surprise measure S_{k+1}

[16] lies in a pre-determined $[T_1, T_2]$ interval. Depending on whether the dictionary remains changed or new data is added, different KRLS update equations are used to update the kernel matrix $\mathbf{K}_{k+1}$, the covariance matrix $\mathbf{P}_{k+1}$ and the weight vector ρ_{k+1} [12], [16]. With the updated matrices and weights, the spatial data component at time instant $k+1$ can be computed.

Combining the prediction results of both components, we can obtain the overall prediction $\hat{x}_{k+1|k} = \hat{x}^{\text{ns}}_{k+1|k} + \hat{x}^{s}_{k+1|k}$. A more in-depth explanation on the algorithm steps and the validation results of this identification algorithm can be found in [12].

III. NONLINEAR MPC IMPLEMENTATION

The goal of the nonlinear model predictive (NMPC) implementation in this project is to obtain the best trade-off between power consumption, and temperature increase while satisfying the system constraints. NMPC implementation in this paper solves for model outputs and control inputs for the future horizon of length N at time instant k. Stacked model outputs and control inputs for the future horizon of length N are shown below:

$$\begin{aligned} X &= \begin{bmatrix} x_k^T & x_{k+1}^T & \dots & x_{k+N}^T \end{bmatrix}, \\ U &= \begin{bmatrix} u_k^T & u_{k+1}^T & \dots & u_{k+N}^T \end{bmatrix} \end{aligned} \tag{6}$$

The first step in NMPC implementation is to construct the nonlinear optimization program for the NMPC implementation.

A. Formulation of the Nonlinear Optimal Control Problem

The optimal control problem considered in this paper can be written as a nonlinear program (NLP) with constraints to be solved at each iteration as follows:

$$\begin{gathered} \text{NLP}(\hat{x}_k, x^{\text{ref}}, u^{\text{ref}}) = \arg\min_{x_k, u_k} l(x_k, u_k) + \rho_k \\ \text{s.t.} \quad x_1 = \hat{x}_k, \\ x_{i+1} = f(x_i, u_i), \quad i = 2, \dots, N \\ 0 \le u_i \le u_{\max} \\ x_i \le T_{\max} \end{gathered} \tag{7}$$

where $T_{max} = 37.8^{\circ}C$ and $u_{max} = 0.065W$. $l(x_k, u_k)$ is the quadratic stage cost. At the time instant k, the cost $l(x,u)$ can be formulated as follows:

$$l(x,u) = \frac{1}{2} \sum_{i=1}^{N} \begin{bmatrix} x_i - x^{\text{ref}} \\ u_i - u^{\text{ref}} \end{bmatrix}^T V \begin{bmatrix} x_i - x^{\text{ref}} \\ u_i - u^{\text{ref}} \end{bmatrix} \tag{8}$$

where i refers to the ith row in the control horizon, V is a symmetric positive semi-definite matrix, x^{ref} consists of a set-point reference value for model outputs, i.e. $x^{\text{ref}} = 37^{\circ}C$, and u^{ref} contains the set-point reference values for model inputs, which is set to $u^{\text{ref}} = 0.065W$.

Nonlinear MPC then solves for

$$(x,u) = \text{NLP}(\hat{x}, x^{\text{ref}}, u^{\text{ref}}) \tag{9}$$

where $u^{\text{NMPC}} = u_1$ are the desired control inputs obtained by the NMPC.

B. Interior Point Algorithm

The interior point algorithm described in [17], [18] combines line search and safeguarding trust region steps to handle non-convexity and to prevent convergence of the solution to non-stationary points. Thus, this interior point algorithm with safeguarding trust region steps is used to approximate and solve the nonlinear problem (7).

This nonlinear model predictive control with interior-point method is implemented in MATLAB using "fmincon" solver, a function for specifying and solving constrained nonlinear optimization programs. The future horizon for prediction and control is set to be of length $N = 10$ to extend the horizon while ensuring that the solver returns a NMPC solution within the time required for real-time control. Based on multiple simulation studies and numerical analysis, the weight matrix V in the objective function is constructed as $V = \begin{bmatrix} 5 \cdot \mathbf{I} & \mathbf{0} \\ \mathbf{0} & 4.5 \cdot \mathbf{I} \end{bmatrix}$ so that the cost function becomes $l(x,u) = \frac{1}{2}\sum_{i=1}^{N} 5(x_i - x^{\text{ref}})^T (x_i - x^{\text{ref}}) + 4.6(u_i - u^{\text{ref}})^T (u_i - u^{\text{ref}})$.

IV. SIMULATION STUDIES

A. Simulation Setup

Simulation studies are run using the multiphysics modeling software COMSOL interfaced with MATLAB similar to previous papers [12] and [19]. Thermal dynamics of the UEA, presented in [13], with multiple heat sources are modeled in the COMSOL software as shown in Fig. 2. The simulation board of the UEA consists of two heat sources and six probes placed surrounding the heat sources to measure the temperature change as further explained in [12]. Power consumption of the UEA falls within the range between 0.04 W and 0.065 W during active operation and 0 W in the sleep mode. 65% of the consumed power is assumed to dissipate into the surrounding tissue as heat and thus, the upper limit for the temperature readings is set to be $0.8^{\circ}C$ above the body temperature, i.e. $37.8^{\circ}C$.

The COMSOL software is interfaced with MATLAB via LiveLink to send control inputs to COMSOL and obtain real-time temperature reading data from COMSOL.

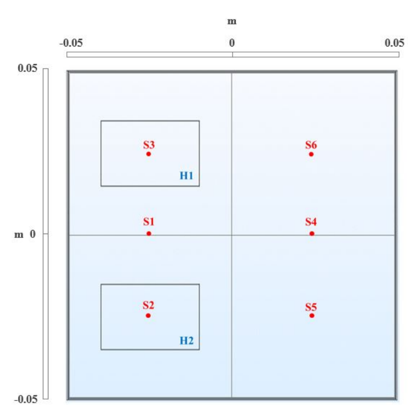

Fig. 2: PCB layout in COMSOL software with sensors locations in *red* (taken from [[12]]).

Prior to simulation studies, a preparation phase is conducted, in which the open-loop system is run for $t = 600$ sec. The goal of this preparation phase is to achieve full convergence of the adaptive filters in the identification algorithms and thus, to minimize the prediction error. During this preparation phase, the power inputs are set to 0.04 W for 10 sec at $t = \{0, 200, 400\}$ sec to excite the system three times and set to 0 W for the rest of the time to prevent any overheating. Results of this preparation phase are shown in Figure 3.

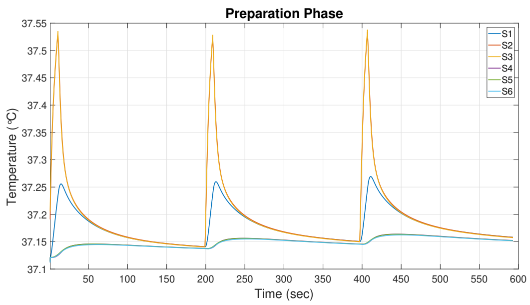

(a)

Fig. 3: Plot of temperature readings in the preparation phase.

B. Simulation Results

A simulation study is conducted to evaluate the performance of the nonlinear model predictive control implementation with the identification algorithm using the COMSOL model. A batch data with randomly generated inputs are from a previous COMSOL simulation is used for data preprocessing, which includes initialization of system matrices and the Kalman gain, computation of threshold values for the surprise criterion and calculation of trends for the spatial and non-spatial data components. The study has been run for 1000 data points to assess the closed-loop behavior of the system under NMPC. Results of this simulation study are shown in Figure 4. More specifically, the power inputs are displayed in Figure 4(a), and the temperature readings corresponding to sensor locations are shown in Figure 4(b). Results shown in Figure 4 demonstrate that the temperature readings are within the bounds of $37 - 37.8^{\circ}C$ and the power inputs solved via the NMPC scheme are also within the bounds of $0 - 0.065W$. The performance of the NMPC implementation with the interior-point method is measured by calculating the mean square of difference between the calculated power levels and the maximum power levels. The mean square difference of the power levels from the maximum levels is 0.062 and 0.060 for power inputs u_1 and u_2, respectively. Additionally, the solver returns a solution in 0.492 sec per sampling iteration on average, which is below the time required per iteration, since the sampling time for each iteration is 1 sec. However, the maximum computation time NMPC scheme requires is 1.631 sec which exceeds the sampling time limit. According to the simulation results, for 75 data points out of 1000 data points total, the sampling time limit has been exceeded. As a result of this, in order to obtain an NMPC scheme suitable for real-time applications, further modifications are necessary, such as increasing the step size, obtaining a suboptimal NMPC solution via early termination to reduce computational cost, implementing a real-time iteration scheme, and so on.

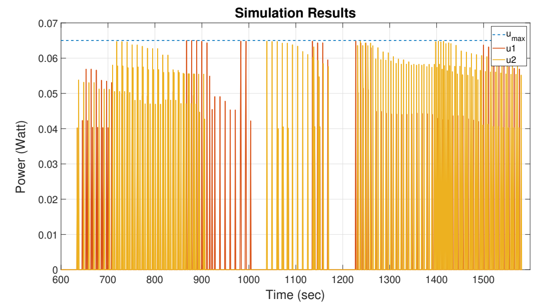

(a)

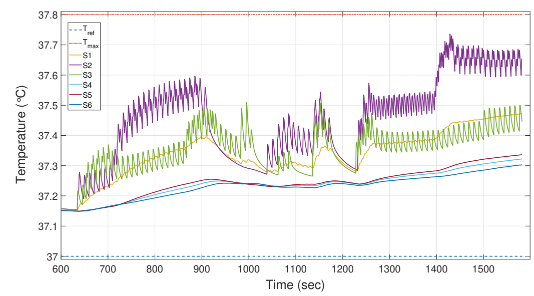

(b)

Fig. 4: (a) Closed-loop simulation results for control inputs, (b) Closed-loop simulation results of temperature readings under the NMPC scheme with interior point method.

In addition to the aforementioned COMSOL simulation study, the NMPC implementation with the interior-point method is compared with a slightly modified version of the method adopted in [9] to evaluate its performance. This method adopts a dual mode control scheme in which the UEA starts at the maximum power level and it is turned off fully when the temperature readings reach $37.8^{\circ}C$. After the temperature readings drop back to $37.3^{\circ}C$ at the sensor locations where the temperature readings reached $37.8^{\circ}C$, the power levels are set back to the maximum level. During its operation, the UEA is either functioning at maximum power levels or it is completely off. The comparison between the NMPC implementation with the interior-point method and the on-off control scheme is shown in Figure 5.

For the modified on-off control method which is implemented for comparison, the mean square difference of the power levels from the maximum levels is $0.059W$ for each power inputs. Compared to the on-off control approach, the NMPC scheme returns relatively similar mean square difference values of the power levels from the maximum level, which are 0.062 and 0.059 for power inputs u_1 and u_2, respectively. Although the mean square difference values for power levels from the reference power level is slightly higher in the NMPC scheme, the simulation results of the NMPC scheme shows that the boundary condition for temperature

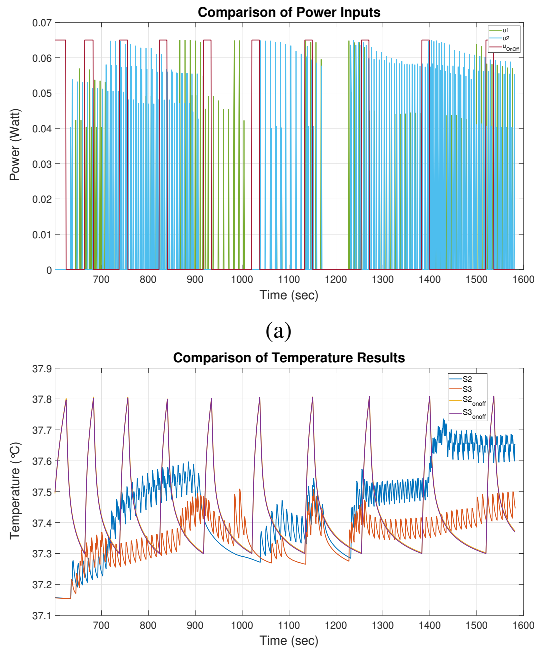

(a)

(b)

Fig. 5: (a) Comparison results for control input u_1 and u_2, (b) Comparison results of temperature readings at sensor locations S2 and S3.

readings, i.e. $x_i \leq T_{\max} = 37.8^{\circ}C$ is satisfied at all times, and the temperature readings never exceed $T_{\max}$. However, the modified on-off control method fails to satisfy this boundary condition for 10 data points out of 1000 data points where the temperature readings exceed $T_{\max}$. Thus, a safe operation of the device is ensured with the NMPC scheme.

V. CONCLUSION

Thermal management of implantable medical devices remains to be an important challenge. In this paper, we investigated utilizing nonlinear model predictive control scheme with the interior-point algorithm to ensure safe operation of IMDs with multiple heat sources. Different from the previous work, which focuses mainly on the thermal management of an IMD with a single heat source, our paper examines the thermal management of an IMD with multiple heat sources. To validate the prediction algorithm, a COMSOL model of the implantable device is created. COMSOL simulation study demonstrates that after the convergence of the adaptive filters of the prediction algorithm, the NMPC scheme with the interior-point method successfully maintains safe temperature levels while optimizing the power inputs. Performance of the investigated control scheme is measured by calculating the square difference of the power inputs from the maximum power levels to determine the deviation from the maximum levels. Although the preliminary results are promising, there are limitations to the current naive NMPC implementation. Mainly, performance of the real-time implementation is restricted by the computational complexity of the NMPC scheme which could be alleviated by increasing the step size, integrating real-time iteration method to reduce the computation time at each iteration, or via early termination of the NMPC.

REFERENCES

[1] M. Seemann, N. Zech, M. Lange, J. Hansen, and E. Hansen. "Anesthesiological aspects of deep brain stimulation : special features of implementation and dealing with brain pacemaker carriers," *Der Anaesthesist*, vol. 62, issue 7, pp.549-556, 2013. [Article in German]

[2] H. Duffau. "Contribution of cortical and subcortical electrostimulation in brain glioma surgery: Methodological and functional considerationsInterest of cortical and subcortical electrical stimuli in cerebral glioma surgery: methodological and functional considerations," *Clinical Neurophysiology*, vol. 37, issue 6, pp.373 -382, 2007.

[3] N. L. Opie, A. N. Burkitt, H. Meffin, and D. B. Grayden, "Heating of the eye by a retinal prosthesis: modeling, cadaver and in vivo study," *IEEE Transactions on Biomed. Eng.*, vol. 59, pp. 339-345, 2012.

[4] M. Diehl, H. J. Ferrau, N. Haverbeke. "Efficient Numerical Methods for Nonlinear MPC and Moving Horizon Estimation," in *Nonlinear Model Predictive Control*, Berlin, Heidelberg: Springer, 2009, vol. 384, pp.391-417.

[5] B. B. Carlos, T. Sartor, A. Zanelli, G. Frison, W. Burgard, M. Diehl, and G. Oriolo, "An Efficient Real-Time NMPC for Quadrotor Position Control under Communication Time-Delay," *Proc. of the 16th International Conference on Control, Automation, Robotics and Vision (ICARCV)*, 2020.

[6] S. Gros, M. Vukov, M. Diehl, "A real-time MHE and NMPC scheme for wind turbine control," in *Proc. of the 52nd IEEE Conference on Decision and Control*, 2013.

[7] S. Gros, M. Zanon, "Data-Driven Economic NMPC Using Reinforcement Learning," *IEEE Transactions on Automatic Control*, vol. 65, issue 2, pp. 636-648, 2020.

[8] J. Lopez-Sanz, C. Ocampo-Martinez, J. Alvarez-Florez; M. Moreno-Eguilaz, R. Ruiz-Mansilla, J. Kalmus, M. Graeber, and G. Lux, "Nonlinear Model Predictive Control for Thermal Management in Plug-in Hybrid Electric Vehicles," *IEEE Transactions on Vehicular Technology*, vol. 66, issue 5, pp. 3632-3644, 2017.

[9] C. T. Wentz, J. G. Bernstein, P. Monahan, A. Guerra, A. Rodriguez, E. S. Boyden, "A wirelessly powered and controlled device for optical neural control of freely-behaving animals," *Journal of Neural Engineering*, vol. 8, issue 4, 2011.

[10] Y.-K. Lo, R. Hill, K. Chen, and W. Liu, "Precision control of pulse widths for charge balancing in functional electrical stimulation," in *Proc. of 2013 6th International IEEE/EMBS Conference on Neural Engineering (NER)*, 2013.

[11] R. Chai, Y. Zhang, "Adaptive Thermal Management of Implantable Device," *IEEE Sensors Journal*, vol. 19, issue 3, pp.1176 - 1185 2018.

[12] A. Ermis, Y. Lai, Y. Zhang, "Online Predictive Modeling of the Thermal Effect of Bio-Implants With Spatially Distributed Parameters," *IEEE Sensors Journal*, vol. 21, issue 2, pp. 2013-2023, 2021.

[13] S. Kim, P. Tathireddy, R. A. Normann, and F. Solzbacher, "Thermal impact of an active 3-D microelectrode array implanted in the brain," *IEEE Transactions on Neural Systems and Rehabilitation Engineering*, vol.15, no.4, pp.493-501, 2007.

[14] S. C. DeMarco, G. Lazzi, W. Liu, J. D. Weiland, and M. S. Humayun, "Computed SAR and thermal elevation in a 0.25-mm 2-D model of the human eye and head in response to an implanted retinal stimulator-Part I: Models and methods," *IEEE Transactions on Antennas and Propagation*, vol.51, no.9, pp.2274-2285, 2003.

[15] I. Houtzager, J. van Wingerden, and M. Verhaegen, "Recursive Predictor-Based Subspace Identification With Application to the Real-Time Closed-Loop Tracking of Flutter," *IEEE Transactions on Control Systems Technology*, vol. 20, issue 4, pp.934 - 949, 2012.

[16] W. Liu, J. C. Principe, and S. Haykin, *Kernel Adaptive Filtering: A Comprehensive Introduction*, John Wiley & Sons, Inc., 2010.

[17] R. H. Byrd, J. C. Gilbert, and J. Nocedal, "A trust region method based on interior point techniques for nonlinear programming," *Mathematical Programming*, vol. 89, pp. 149-185, 2000.

[18] R. A. Waltz, J. L. Morales, J. Nocedal, and D. Orban, "An interior algorithm for nonlinear optimization that combines line search and trust region steps," *Mathematical Programming*, vol. 107, pp. 391-408, 2006.

[19] A. Ermis, Y. Lai, X. Pan, R. Chai, and Y. Zhang, ”Recursive Subspace Identification for Online Thermal Management of Implantable Devices,” *Proc. of 57th Allerton Conference on Communication, Control, and Computing*, 2019.